Characterization of Chondroitin Sulfate Lyase ABC from *Bacteroides thetaiotaomicron* WAL2926[†]

David Shaya,[‡,#] Bum-Soo Hahn,[§,#] Nam Young Park,[||] Joon-Soo Sim,[§] Yeong Shik Kim,[||] and Miroslaw Cygler*[,‡,⊥]

Department of Biochemistry, McGill University, Montreal, Quebec, Canada, National Institute of Agricultural Biotechnology, 225 Seodun-Dong, Suwon 441-707, South Korea, Natural Products Research Institute, College of Pharmacy, Seoul National University, Seoul 151-742, South Korea, and Biotechnology Research Institute, NRC, 6100 Royalmount Avenue, Montréal, Québec, Canada H4P 2R2

Received February 29, 2008; Revised Manuscript Received May 14, 2008

ABSTRACT: Chondroitin sulfate ABC lyase (ChonABC) is an enzyme with broad specificity that depolymerizes via β-elimination chondroitin sulfate (CS) and dermatan sulfate (DS) glycosaminoglycans (GAGs). ChonABC eliminates the glycosidic bond of its GAG substrates on the nonreducing end of their uronic acid component. This lyase possesses the unusual ability to act on both epimers of uronic acid, either glucuronic acid present in CS or iduronic acid in DS. Recently, we cloned, purified, and determined the three-dimensional structure of a broad specificity chondroitin sulfate ABC lyase from *Bacteroides thetaiotaomicron* (BactnABC) and identified two sets of catalytic residues. Here, we report the detailed biochemical characterization of BactnABC together with extensive site-directed mutagenesis resulting in characterization of the previously identified active site residues. BactnABC's catalysis is stimulated by Ca^{2+} and Mg^{2+} cations, particularly against DS. It displays extremely low activity toward hyaluronic acid and no activity toward heparin/heparan sulfate. Degradation of CS and DS by BactnABC yields only disaccharide products, pointing to an exolytic mode of action. The kinetic evaluations of the active-site mutants indicate that CS and DS substrates bind in the same active site, which is accompanied by a conformational change bringing the two sets of active site residues together. Conservative replacements of key residues suggest that His345 plays the role of a general base, initiating the degradation by abstracting the C5 bound proton from DS substrates, whereas either Tyr461 or His454 perform the equivalent role for CS substrates. Tyr461 is proposed, as well, to serve as general acid, completing the degradation of both CS and DS by protonating the leaving group.

Glycosaminoglycans are highly sulfated, linear polysaccharides composed of alternating hexosamine (glucosamine or galactosamine) and uronic acid (D-glucuronic or L-iduronic) moieties. Most GAGs[1] are linked through a serine residue to a core protein forming a proteoglycan (PG). PGs are ubiquitous within the extracellular matrix (ECM) and are present on the cell surfaces of vertebrates. Through their interaction with a wide variety of proteins, PGs modulate fundamental biological processes including cell adhesion, proliferation, differentiation, signaling, inflammation, and infection (*1*–*8*).

Dermatan sulfate (DS) and chondroitin sulfate (CS) are structurally related GAGs, composed of alternating 1,4-β-D-*N*-acetylgalactosamine (GalNac) and 1,3-α-L-iduronic acid (DS) or 1,3-β-D-glucuronic acid (CS) (*5, 9*). The uronic acid moiety in CS is exclusively β-D-glucuronic acid (GlcA), whereas DS contains a mixture of α-L-iduronic acid (IdoA) and GlcA epimers (Figure 1) (*10*). During their biosynthesis, CS and DS polysaccharides undergo sulfation at various positions, generating their chemical diversity. Chondroitin sulfate is primarily characterized by *O*-sulfation at either the C4 position (chondroitin 4-sulfate, CS-A) or the C6 position (chondroitin 6-sulfate, CS-C) of GalNac, whereas DS is primarily sulfated at the C4 position of the galactosamine. Additional, less frequent *O*-sulfation is found at the C2 position of IdoA in DS, creating disulfated disaccharide units that have been implicated in regulating the biological functions of this polymer (*3*).

Specialized microorganisms express GAG-degrading lyases using their terminal products as a source of carbon. Unlike the eukaryotic GAG hydrolases, these prokaryotic enzymes depolymerize GAGs through a β-elimination mechanism characterized by the removal of a relatively acidic proton from the C5 carbon (the chiral center) of the uronic

[†] This research was supported by the Canadian Institutes of Health Research (CIHR) grant MOP-74725 to M.C., by the KOSEF grant RO1-1999-2-209-010-5 to Y.S.K., and by the grant from National Institute of Agricultural Biotechnology to B.-S.H.

* Corresponding author. Phone: 514-496-6321. Fax: 514-496-5143. E-mail: mirek.cygler@bri.nrc.ca.

[‡] McGill University.

[§] National Institute of Agricultural Biotechnology.

[||] Seoul National University.

[⊥] NRC.

[#] These authors contributed equally to this paper.

[1] Abbreviations: GAG, glycosaminoglycan; CS, chondroitin sulfate; DS, dermatan sulfate; CS-A, chondroitin 4-sulfate; CS-C, chondroitin 6-sulfate; GalNAc, *N*-acetyl-D-galactosamine; GlcA, β-D-glucuronic acid; IdoA, α-L-iduronic acid; ChonABC, chondroitin sulfate ABC lyase; BactnABC, chondroitin sulfate ABC lyase from *Bacteroides thetaiotaomicron*; PvulABCI, chondroitin sulfate ABC I lyase from *Proteus vulgaris*; PvulABCII, chondroitin sulfate ABC II lyase from *Proteus vulgaris*.

10.1021/bi800353g CCC: $40.75
Published on Web 05/31/2008

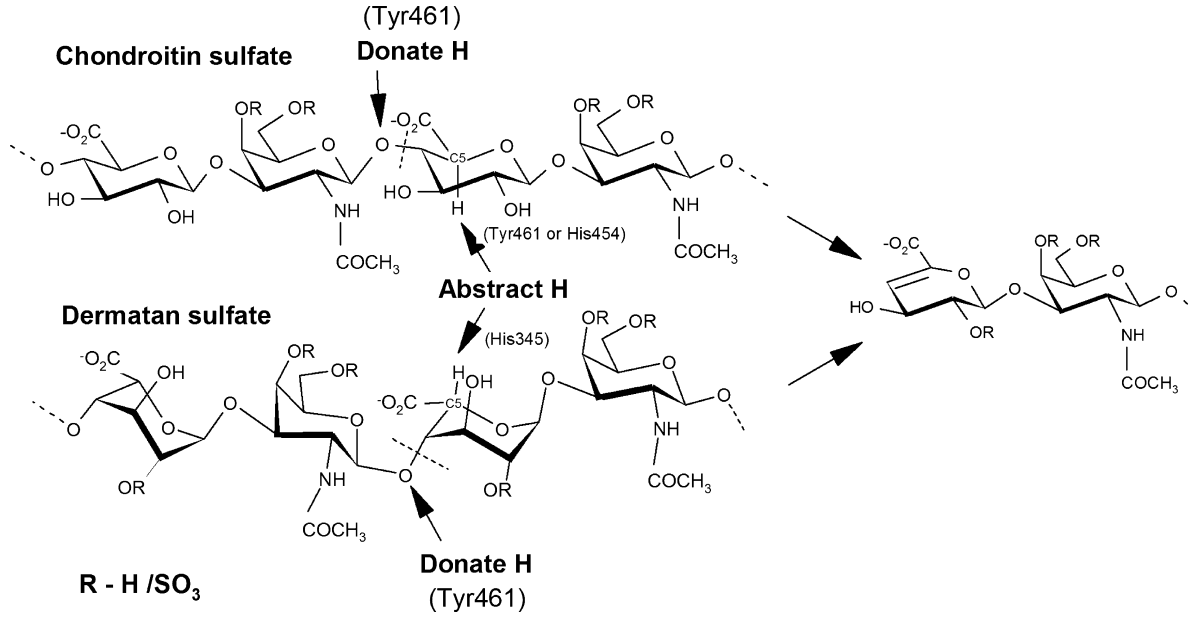

FIGURE 1: Chemical schemas of CS and DS degradation.

acid, and the release of the 4-linked hexosamine with the generation of a C4−C5 double bond at the uronic acid ring (*11*) (Figure 1). During the past two decades, GAG lyases have found uses as tools to dissect the complex structure of GAG polysaccharides (*12*). The broad specificity of ChonABC from the bacterium *Proteus vulgaris*, depolymerizing both CS and DS, was recently shown to enhance axonal regeneration and improve nerve plasticity following spinal cord injury in model systems (*13, 14*). Similar broad specificity of ChonABC lyases have been identified in the genome of *Bacteroides thetaiotaomicron* (*15*). A thorough biochemical characterization of this enzyme, together with a simple expression−purification protocol, could offer novel therapeutic tools to overcome debilitating spinal cord injury.

ChonABC was initially identified in the gram-negative bacterium *Proteus vulgaris*. Two orthologues, the endolytic PvulABCI (gi:1095454, MW of 115.2 kDa and 1,021 amino acids) and the exolytic PvulABCII (gi:1828879, with MW of 114.1 kDa and 1,013 amino acids), were biochemically characterized (*16, 17*). We have previously determined the crystal structure of PvulABCI (*18*). Continuing our efforts to explain the enzyme's broad substrate specificity and its mechanism of action, we recently cloned, expressed, and determined the structure of chondroitinase ABC from the gram-negative *Bacteroides thetaiotaomicron* WAL2926 (BactnABC, MW of 115.2 kDa and 1,016 amino acids; sequence in Supporting Information, Table S2). Comparison of the structures of these two enzymes led to the identification of two clusters of essential active site residues: in addition to the Tyr461-His454-Glu628-Arg514 tetrad, we have identified His344, His345, and Arg172, located on the opposite rim of the substrate binding site, as affecting significantly catalytic activity (*19*). We present here the biochemical characterization of BactnABC, providing conditions for optimal activity, and report the enzyme's product profile against a broad spectrum of GAG substrates. We performed an extensive mutational analysis of the residues implicated in activity, using both short-term kinetic assays and overnight end-point product formation assays to confirm their functional roles in catalysis.

MATERIALS AND METHODS

Site-Directed Mutagenesis of BactnABC. Genomic DNA was isolated from cultures of *Bacteroides thetaiotaomicron* strain WAL2926 (Korean Culture Center of Microorganisms), and the gene BT3324 (gi: 29348733) was subcloned into the expression vector pET-22b (Novagen) with a C-terminal His_6 tag as described previously (*19*). DNA sequencing revealed 16 amino acid differences (Supporting Information, Table S1) with the published sequence (gi: 166235375) related to strain differences between the WAL2926 and the VPI-5482 isolates (NCBI deposited sequence). BactnABC mutants were constructed using the QuickChange Site-Directed Mutagenesis Kit (Stratagene), according to the manufacturer's protocol, using DNA primers listed in Table S2 (Supporting Information) and their sequences confirmed by DNA sequencing. The mutants were expressed in *E. coli* BL21 (DE3).

Purification of Recombinant BactnABC. Recombinant BactnABC and derived mutant enzymes were expressed in *E. coli* strain BL21(DE3), which is devoid of GAG lyase activity (*17*), and purified as described earlier (*19*). Briefly, cells expressing BactnABC were cultured in Luria broth at 37 °C supplemented with 100 μg mL^{-1} ampicillin and protein expression induced with 1 mM IPTG. Cells were disrupted by sonication and purified using a combination of DEAE (GE Healthcare), Ni-NTA (Qiagen), Mono-S HR 10/10 (GE healthcare), and HiLoad 16/60 Superdex 200 (GE healthcare) columns. The purity of the eluted fractions was evaluated by SDS−PAGE stained by Coomassie Blue R-250, which showed a single band on an overloaded gel, corresponding to the expected MW of the recombinant enzyme. Fractions containing purified, active BactnABC were pooled, concentrated to 8 mg/mL by ultrafiltration (Centricon YM-50 concentrator, Millipore Corporation) and used in subsequent characterization experiments.

Biochemical Characterization of Recombinant BactnABC. BactnABC Activity. BactnABC lyase activity was measured on the basis of the increase in absorbance at 232 nm (*20*). One unit of enzyme is the amount required for the

eliminative cleavage of substrate, yielding 1 μmol of UV-absorbing, double bond-containing products per min as calculated using a molar absorption coefficient (ε) of 3800 M^{-1} cm^{-1}. All experiments were carried out in a 1 cm path length quartz cuvette with a total volume of 1 mL and included at least three repetitions. Protein concentrations were determined using the Bradford Protein Assay Reagent kit (Bio-Rad).

Buffer Selection. We first established the appropriate buffer for subsequent biochemical characterizations by comparing enzyme specific activity in Tris versus the phosphate buffer system. Accordingly, 50 mM potassium phosphate, the optimal buffer, was used in the determination of pH and temperature effects on activity, and the optimal pH (7.6) and temperature (37 °C) established were used in subsequent experiments. Since phosphate forms insoluble salts with some metal ions, Tris-HCl buffer was used to determine the influence of ionic strength (sodium chloride and potassium chloride) and divalent metal cations on the activity of the wild-type enzyme.

Substrate Preference. To determine the substrate preferences of the enzyme, 12 GAG substrates from different sources and manufacturers were used: CS-A from bovine trachea (Biocorp), DS from porcine intestinal mucosa (Sigma, Calbiochem), CS-C from shark cartilage (Sigma, Seikagaku), CS-D from skate (unpublished results), CS-E from squid (unpublished results), low molecular weight (100 kDa) and high molecular weight (1400 kDa) hyaluronan from chicken combs (Kibun Food Chemifa Co, Japan), acharan sulfate from giant snail (according to ref *21*), heparin from porcine intestinal mucosa (New Zealand Pharmaceuticals Ltd.), and heparan sulfate from bovine kidney (Seikagaku). Each substrate was dissolved at a concentration of 1 mg mL^{-1} in 50 mM phosphate buffer at pH 7.6. Unless specified otherwise, the reaction was initiated by the addition of 1 μg of wild type BactnABC, and at 232 min^{-1} was recorded over 300 s at 37 °C. Since the chondroitin sulfates substrates, derived from various natural sources, differ in the level and type of substitutions, we have characterized their disaccharide composition by a complete digestion using PvulABC. Disaccharide separation and identification was preformed using FPLC, as described later in the product profile analysis section, and composition analysis was calculated by integrating and comparing the peak areas (mAU min).

Optimal Temperature, pH, Ionic Strength, and Divalent Metal Cations. CS-A (Biocorp), DS (Sigma), and CS-C (Sigma), each at a concentration of 1 mg mL^{-1}, were assayed under various conditions in an attempt to determine the effects of temperature, pH, ionic strength, and divalent metal cations on enzymatic activity. The temperature was varied between 25−50 °C using a temperature-controlled UV spectrophotometer (DU 800, Beckmann-Coulter), and 50 mM phosphate at pH 7.6 was used as the reaction buffer. To determine BactABC's temperature stability, we have remeasured the activity at 37 °C after preincubation for 5 min at each temperature in the 25−50 °C range. The influence of pH on activity was investigated in 50 mM phosphate buffer at pH 6−9. The relative effects of ionic strength, divalent metal ions, and titration of Ca^{2+} cations were measured in Tris-HCl buffer. The protein was dialyzed into 50 mM Tris-HCl at pH 7.6, and increasing concentrations of sodium, potassium, and calcium chloride were added to the reaction. To evaluate the effect of divalent metal ions on the activity of BactnABC, a constant concentration of various metal chloride salts (10 mM) was added to the reaction.

Determination of Apparent T_m. A fluorescence microplate reader (FluoDia T70, Photon Technology International) was used to monitor the thermal denaturation of BactnABC and PvulABC using SYPRO orange fluorescence as a readout (*22, 23*). PvulABC was purchased from Seikagaku. A final concentration of 2 μM protein combined with SYPRO Orange (Invitrogen) in reaction volumes of 25 μL was incubated in 50 mM phosphate, pH 7.6, and 50 mM Tris-HCl, pH 7.6, respectively. The temperatures were varied between 23−75 °C using 1 °C steps. The samples were excited at 465 nm and the fluorescence emission recorded at 590 nm. The data was interpreted using the Levenberg−Marquardt nonlinear regression algorithm (Octave, http://www.octave.org). The inflection point (apparent T_m) was determined by fitting the data to the equation $f(T) = A + (B - A)/(1 + \exp(T_m - T)/C)$, where A is the fluorescence minimum, B is the fluorescence maximum, C is the rate of fluorescence change around the inflection point, and T is the temperature.

Kinetic Analysis. The kinetic parameters of BactnABC and its mutants toward CS-A (Biocorp), DS (Sigma), and CS-C (Sigma) were determined spectrophotometrically. Various quantities of substrate (0.1−5 mg) were dissolved in 50 mM phosphate at pH 7.6, at 37 °C, and the initial reaction rates were recorded within 1 to 5 min. The data were interpreted using linear regression analysis (Hyper Version 1.0.0 http://wvlc.uwaterloo.ca/biology447/modules/module7/hyper/index.htm). The kinetic parameters (k_{cat} and K_M) were determined by fitting the data to the equation: $[S]/v = K_M/V_m + [S]/V_m$ (Hanes plot), where K_M represents the substrate concentration at half-saturation. The k_{cat} value was calculated using the equation $V_{max} = k_{cat} \times [E]$, where [E] represents total enzyme concentration.

Product Profile Analysis. The product profiles resulting from the exhaustive digestion of various substrates by BactnABC and its corresponding mutant enzymes were analyzed using strong anion-exchange high performance liquid chromatography (SAX-FPLC). For each reaction, 0.5 mg of CS-A (Biocorp), DS (Sigma), or CS-C (Sigma) were enzymatically depolymerized using 0.25, 0.75, and 0.5 μg of enzyme respectively, in total volumes of 500 μL of 50 mM phosphate at pH 7.6. The reactions were incubated overnight at 37 °C and terminated by heating for 5 min at 100 °C. Samples were applied to a Hypersil SAX column (250 × 4.6 mm, 5 μm, Bellefonte, PA, USA) operated using an ÄKTA purifier FPLC (GE Healthcare). The column was washed with one column volume of water (pH 3.5, adjusted with HCl), and a linear gradient of 0−1.0 M NaCl (pH 3.5, adjusted with HCl) over 10 column volumes was used to separate the products. Disaccharide standard mixtures (Seikagaku), analyzed in the same manner, were used to identify the digestion products by comparing retention times.

RESULTS

Biochemical Characterization of BactnABC. Buffer Effects on Activity. Previous reports showed that the enzymatic activity of BactnABC is strongly influenced by the buffer used. Linn

Table 1: Specific Activity of BactnABC Acting on Various GAG Substrates[a]

substrate	average MW (kDa)	specific activity (U/mg of protein)	relative activity (%)	ΔDi-0S (%)	ΔDi-6S (%)	ΔDi-4S (%)	ΔDi-2,6 diS (%)	ΔDi-4,6 diS (%)	ΔDi-2,4 diS (%)
CS-A bovine trachea (Biocorp)[b]	12	77.6 ± 1.1	100	5.4	9.2	74.7	0.4	0.3	0
DS porcine intestinal mucosa (Sigma)[b]	16	9.1 ± 0.8	11.7	1.4	5.5	85.7	0.7	6.7	0
DS porcine intestinal mucosa (Calbiochem)[b]	20	12.5 ± 0.9	16.1	23.8	6.1	63.7	0	5.2	1.2
CS-C shark cartilage (Sigma)[b]	35	47.4 ± 0.8	61.1	2.8	46.4	31.2	18.2	0.7	0.7
CS-C shark cartilage (Seikagaku)[b]	39	18.2 ± 1.0	23.4	4.1	61.1	21.5	13.1	0.2	0
CS-D skate cartilage[b,e]	44	14.4 ± 0.4	18.5	2.5	40.5	35.6	20.7	0.1	0.6
CS-E squid cartilage[b,f]	97	28.5 ± 0.8	36.7	13.0	22.1	45.8	0	19.1	0
low molecular weight Hyaluronic acid (Kibun Food Chemifa)[c]	100	0.8 ± 0.1	1.1						
high molecular weight Hyaluronic acid (Kibun Food Chemifa)[d]	1400	0.2 ± 0.1	0.2						
acharan sulfate [d,g]		n.d.	n.d.						
heparin (New Zealand Pharmaceuticals)[d]		n.d.	n.d.						
heparan sulfate (Seikagaku)[d]		n.d.	n.d.						

[a] One mg mL^{-1} of each substrate was dissolved in 50 mM phosphate at pH 7.6 and the reaction monitored for 300 s at 37 °C following the addition of the enzyme. The values for the specific activities are the mean ± S.D. of at least three measurements. Disaccharide compositions of the substrates are ΔDi0S = ΔUA-GalNAc; ΔDi6S = ΔUA-GalNAc6S; ΔDi4S = ΔUA-GalNAc4S; ΔDi2,6 diS = ΔUA2S-GalNAc6S; ΔDi4,6 diS = ΔUA-GalNAc4S6S; ΔDi2,4 diS = ΔUA2S-GalNAc4S. n.d., not detected; less than 0.1% of WT activity. [b] 1.0 μg of WT BactnABC was used in the assay. [c] 7.5 μg WT BactnABC was used in the assay. [d] 15 μg WT BactnABC was used in the assay. [e] CS-D was purified from skate cartilage. [f] CS-E was purified from squid cartilage. [g] Acharan sulfate was purified from giant snail according to ref *21*.

Table 2: Specific Activity of BactnABC in the Presence of Divalent Cations[a]

divalent cation	specific activity (U/mg)		
	CS-A	CS-C	DS
50 mM phosphate (pH 7.6)	77.6 ± 1.1	47.4 ± 0.8	9.1 ± 0.8
50 mM Tris-HCl (pH 7.6)	12.3 ± 0.7	8.1 ± 0.5	0.1 ± 0.1
+10 mM $CaCl_2$	28.2 ± 1.0	14.6 ± 0.9	4.5 ± 0.3
+10 mM $MgCl_2$	38.2 ± 0.4	19.3 ± 0.8	5.2 ± 1.8
+10 mM $MnCl_2$	4.3 ± 1.6	4.0 ± 0.5	0.7 ± 0.2
+10 mM $ZnCl_2$	1.3 ± 0.4	0.9 ± 0.6	0.7 ± 0.2
+10 mM $BaCl_2$	18.6 ± 0.2	10.2 ± 0.6	4.4 ± 0.1
+10 mM CsCl	12.1 ± 0.2	8.2 ± 0.4	0.7 ± 0.1

[a] One mg mL^{-1} CSA (Biocorp)/CSC (Sigma)/ DS (Sigma) was assayed with 1 μg of BactnABC in 50 mM Tris-HCl (pH 7.6) containing various divalent cations at a final concentration of 10 mM. The values given are the mean ± S.D. for at least three measurements.

and co-workers reported maximal activity for BactnABC in phosphate buffer, while using Tris-HCl buffer required the addition of NaCl (*15*). To establish the appropriate buffer for recombinant BactnABC, we compared its activity in Tris versus the phosphate buffer system. The enzyme activity measured in phosphate is 77.6 U/mg for CS-A, 47.4 U/mg for CS-C, and 9.1 U/mg for DS (Tables 1 and 2). When the activity is measured in Tris-HCl buffer, we observed a ~6-fold lower activity for the CS-A/CS-C substrates, while a much larger, 80-fold decrease was observed for DS (Table 2). Accordingly, 50 mM phosphate was used in the determination of pH and temperature effects on activity.

Temperature Dependence of Activity and Enzyme Stability. The temperature dependence of BactnABC activity and its thermal stability was tested in the range of 25−50 °C (Figure 2). The enzyme displayed no significant reduction in activity at temperatures in the range of 25−40 °C. Maximal activity for all substrates was attained at 37 °C. At lower temperatures, the activity toward DS drops the least (85% at 25 °C), while the activity toward CS-A and CS-C was reduced to 50% and 65%, respectively. However, at higher temperatures the activity toward DS declines faster (45% at 50 °C for DS vs 60% for CS-A and 75% for CS-C). To determine if this decrease of activity above 40 °C is caused in part by irreversible denaturation, we have incubated the enzyme for 5 min at each temperature and transferred the enzyme to 37 °C for activity measurements (Figure 2b). The results indicate that denaturation is, indeed, a factor at temperatures above 40 °C.

We further investigated the temperature stability of BactnABC by fluorescence. We measured the changes in fluorescence of the SYPRO Orange dye as a function of temperature. This fluorophore is sensitive to the change in hydrophobicity of the environment. The increased exposure of hydrophobic regions of the protein during thermal denaturation leads to an increase in the fluorescence emitted from the fluorophore (*24*). Thermal unfolding was measured in two buffers, potassium phosphate and Tris-HCl, at pH 7.6. In both buffers, the fluorescence emission as a function of temperature showed a bimodal melting curve with two inflection points representing two consecutive denaturing events (data not shown). The first T_m corresponds to 44 °C and the second to 50 °C. Thermal denaturation was not visible below 41 °C, in complete agreement with the activity-measured temperature stability (Figure 2b). PvulABC, however, presented a unimodal curve with a T_m of 38 °C for thermal denaturation (data not shown).

Effect of pH on Activity. The pH optimum for BactnABC was determined to be 7.6. The enzyme exhibited a bell-shaped, narrow pH-activity profile of ± ~0.5 pH unit around the optimum, with marked decrease in activity at pH values below 7.0 and above 8.0 (Figure 2b). Interestingly, the activity toward CS-C remained higher than with the other substrates at low pH. Thus, at pH 6.5 the enzyme exhibited almost 60% of its maximal activity toward CS-C, only 20% activity toward CS-A, and no measurable activity toward DS. In contrast, at pH of 8.5 BactnABC displayed ~30% of its maximal activity toward all substrates. Subsequent assays were performed at the optimum pH of 7.6 and at a temperature of 37 °C.

Substrate Preference. To map the substrate preference of BactnABC, we compared the enzyme's specific activity toward a wide range of GAG substrates: CS-A, DS, CS-C, CS-D, CS-E, low and high molecular weight hyaluronic acid, acharan sulfate (AS), heparin, and heparan sulfate (Table 1). The enzyme displayed somewhat different activity toward the same substrate obtained from different suppliers. We have, therefore, analyzed the disaccharide composition of

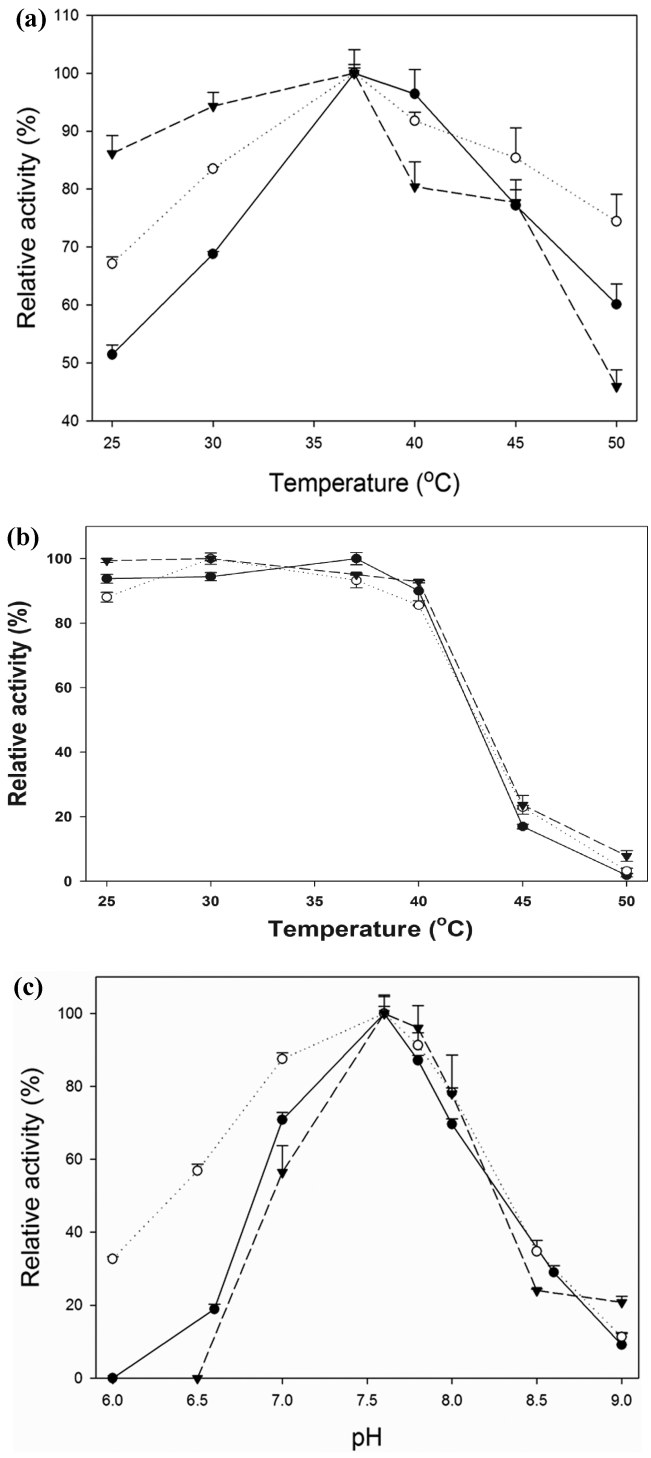

FIGURE 2: Effect of temperature and pH on BactnABC activity. (a) Effect of temperature on BactnABC activity; buffer is 50 mM phosphate at pH 7.6. (b) Temperature stability of BactnABC; buffer is 50 mM phosphate at pH 7.6 at 5 min incubation of BactnABC in temperatures varying 25−50 °C followed by activity measurement at 37 °C. (c) pH effects on BactnABC activity; buffer is 50 mM phosphate with varying pH. All experiments contained 1 mg mL^{-1} of CS-A with 0.5 μg of BactnABC (●), DS with 1.5 μg of BactnABC (▼), and CS-C with 1 μg of BactnABC (○).

each substrate by exhaustive digestion with PvulABC and analysis of the disaccharides by FPLC (Table 1), and identified the content of various substitutions. The differences were relatively small for DS but substantially larger for CS-C, reflecting different levels of 4-*O*-sulfation in CS-C from Sigma compared to CS-C from Seikagaku. CS-E resembles the disaccharide composition of CS-A as compared to CS-D, which resembles the composition of CS-C from Sigma. BactnABC is highly active toward chondroitin substrates, whereas it shows no activity toward heparin substrates (AS, heparin and heparan sulfate; Table 1).

Mode of Action. To determine whether BactnABC acts in an endolytic or exolytic manner, we examined the product profile of BactnABC using SAX-FPLC. We observed only disaccharide products for each of the substrates tested (Figure 3). CS-A and DS digestion afforded three disaccharide products ΔUA-GalNAc4S, ΔUA-GalNAc6S, and ΔUA-GalNAc (ΔUA-4,5 unsaturated uronic acid) with the 4-sulfated disaccharide being the major product (Figure 3b). The profile for digestion of CS-C revealed the same three products with the 6-sulfated disaccharide being the major product (Figure 3c). CS-C digestion also yielded the disulfated disaccharide product ΔUA2S-GalNAc6S. No tetrasaccharide products were found during the course of digestion, consistent with an exolytic mode of action for this enzyme.

Effect of Ions on Activity. The concentration of mono and divalent ions had a clear effect on enzyme activity. These measurements were performed in Tris-HCl buffer. For the monovalent ions tested, increasing the concentration of sodium, potassium, or cesium chloride from 0 to 0.1 M increased the activity against all substrates (Figure 4a−c). Further increases in salt concentration reduced the activity dramatically, with 50% inhibition occurring at ∼0.15 M and a nearly complete inhibition at 0.4 M salt. This general effect of ionic concentration on BactnABC's activity likely explains the elevated activity in the phosphate buffer versus that of the Tris-HCl buffer.

We have previously demonstrated that Ca^{2+}/Mg^{2+} cations play a role in catalysis, especially pronounced in the case of DS (*19*). We continued investigating the effect of other divalent ions, Mn^{2+}, Zn^{2+}, on the activity of BactnABC. As reported earlier, the addition of 10 mM Ca^{2+} or Mg^{2+} ions increased the activity toward CS-A/CS-C by 2−3-fold, while the activity toward DS increased much more significantly by 50-fold (Table 2). Addition of Mn^{2+} and Zn^{2+} reduced the activity against CS substrates but increased the activity toward DS (Table 2).

Effect of Ca^{2+} on Activity. Having demonstrated the importance of Ca^{2+} for degradation, we further investigated the effect of this cation on the activity of BactnABC. The addition of $CaCl_2$ to the reaction mixture had a different effect on CS degradation compared to DS degradation. The activity profile recorded with CS substrates was comparable to the effect observed with monovalent ions. Thus, increasing the concentration of $CaCl_2$ with both CS-A and CS-C from 0 to 0.04 M increased the activity, as in the case of the monovalent ions (Figure 4d). A further increase of $CaCl_2$ concentration reduced the activity, with 50% inhibition at ∼0.065−0.085 M and a complete inhibition of the reaction at 0.2 M. The activity with DS displayed a different behavior as a function of Ca^{2+} concentration, indicating a different role for Ca^{2+} with this substrate. The addition of a low concentration of $CaCl_2$ dramatically increased the activity from a basal level. The maximal activity was reached at 0.01 M $CaCl_2$ (Figure 4d and Table 2). Further increasing the $CaCl_2$ concentration resulted in a behavior similar to that with other salts. A similar, specific effect on DS degradation was also observed with Ba^{2+} (Figure 4e).

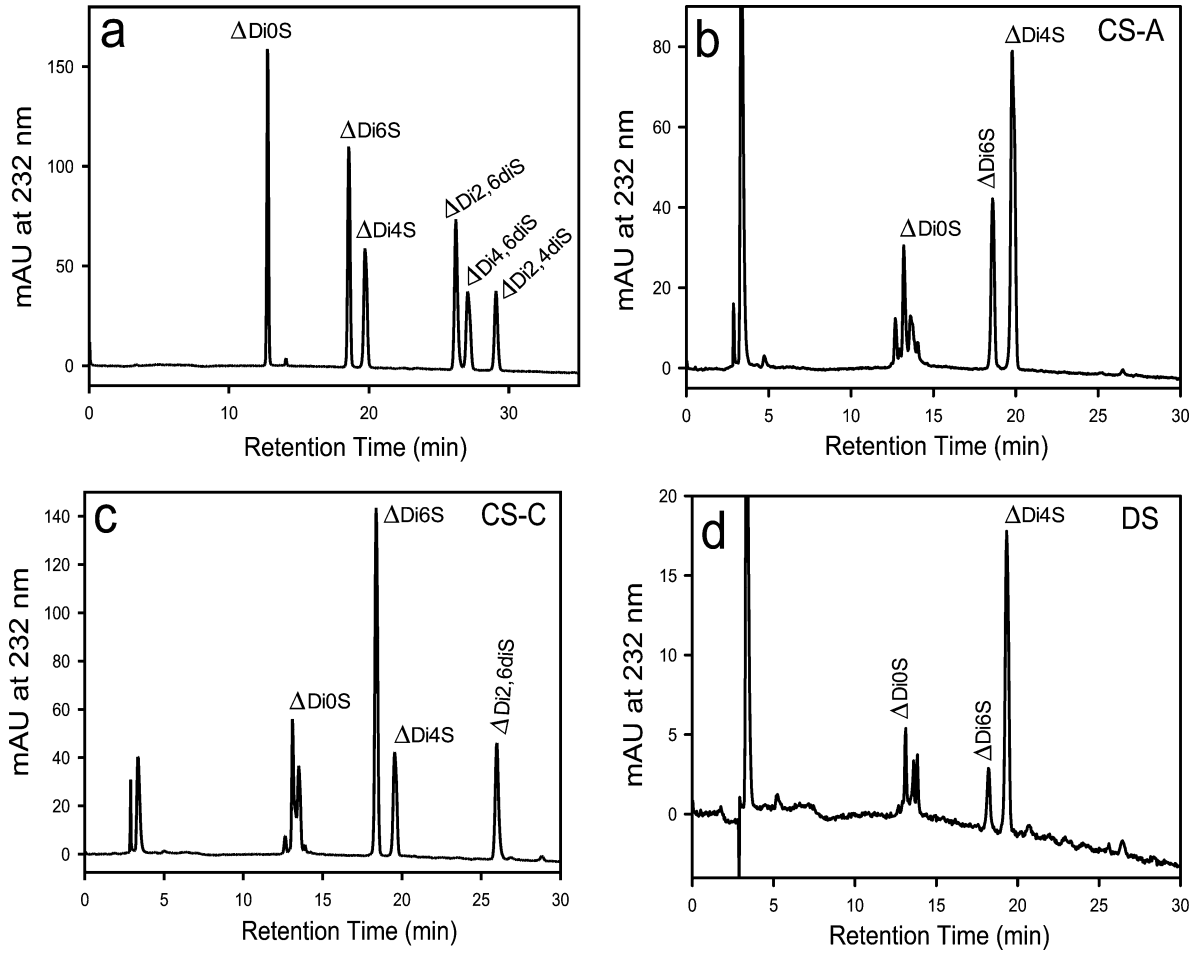

FIGURE 3: Product profile analysis using SAX-FPLC. (a) Disaccharide standard mixtures from Seikagaku. Degradation profiles of wild-type BactnABC acting on (b) Biocorp CS-A, (c) Sigma CS-C, and (d) Sigma DS. Disaccharides identified: ΔDi0S = ΔUA-GalNAc; ΔDi6S = ΔUA-GalNAc6S; ΔDi4S = ΔUA-GalNAc4S; ΔDi2,6diS = ΔUA2S-GalNAc6S; ΔDi4,6diS = ΔUA-GalNAc4S6S; ΔDi2,4diS = ΔUA2S-GalNAc4S.

Kinetic Analysis of Active-Site Mutants. Using alanine-scanning site-directed mutagenesis, we previously identified two groups of amino acids involved in catalysis (*19*). In order to characterize the specific catalytic roles of these residues, we have investigated the effects of conservative and non-conservative mutations on BactnABC activity. The first group of residues was identified by structural similarity to the active site of chondroitinase AC. Following the nomenclature used for chondroitinase AC (*25, 26*), we termed His454, Tyr461, Arg514, and Glu628 (Figure 5) the catalytic tetrad (*19*). Mutating any of these residues to an alanine was shown to have an acute effect on the degradation of both CS and DS substrates (*19*). We prepared the H454D mutant in order to ascertain its role as a general base in catalysis. In parallel, we replaced this histidine with an asparagine or a glutamine to evaluate the importance of hydrogen bonds maintained by either of its nitrogen atoms (ND isosteric to -NH_2 of asparagine, and NE isosteric to NH_2 of glutamine) for activity. No detectable activity was observed for any of these mutants (Table 3, Figure 6, and Supporting Information Figure S1). Another residue, Tyr461, was previously proposed to serve as a general base in CS degradation but not DS degradation (*19*). In addition to the previously reported Y461F mutation that rendered the enzyme inactive toward all substrates, we constructed an Y461A mutant enzyme with the reasoning that a water molecule could enter the vacated space and partially replace the -OH group of the tyrosine side chain. However, this mutant also showed no activity. The mutations E628D and E628Q were then prepared in order to examine the role of this residue in maintaining the integrity of hydrogen-bonding interactions among the residues forming the tetrad. The E628D mutant rendered the enzyme inactive; however, an E628Q mutant retained low levels of activity toward CS substrates but not toward DS (Table 3 and Figure 6). Previously, we investigated the functional role of His453, which precedes His454. Replacement of His454 by an alanine moderately reduced the activity toward all substrates (*19*). Surprisingly, the H453N mutant showed no activity toward DS while retaining about 10% of its catalytic efficiency (k_{cat}/K_M) against CS-A and CS-C (Table 3 and Figure 6).The second group of residues includes the basic patch of Arg172, His344, and His345 (Figure 5). These residues were identified by structural conservation between BactnABC and PvulABCI (*19*). These residues are located on the opposite rim of the substrate-binding site ~12 Å from the tetrad and are implicated in the degradation of DS substrates (*19*). We mutated the two histidines to either aspartates or glutamates in order to ascertain their role in catalysis as potential general bases. Replacing either of these two histidine side chains by acidic residues rendered the enzyme inactive toward all substrates (Table 3, Figure 7, and Supporting Information Figure S2). We then replaced each of these histidines by either an asparagine

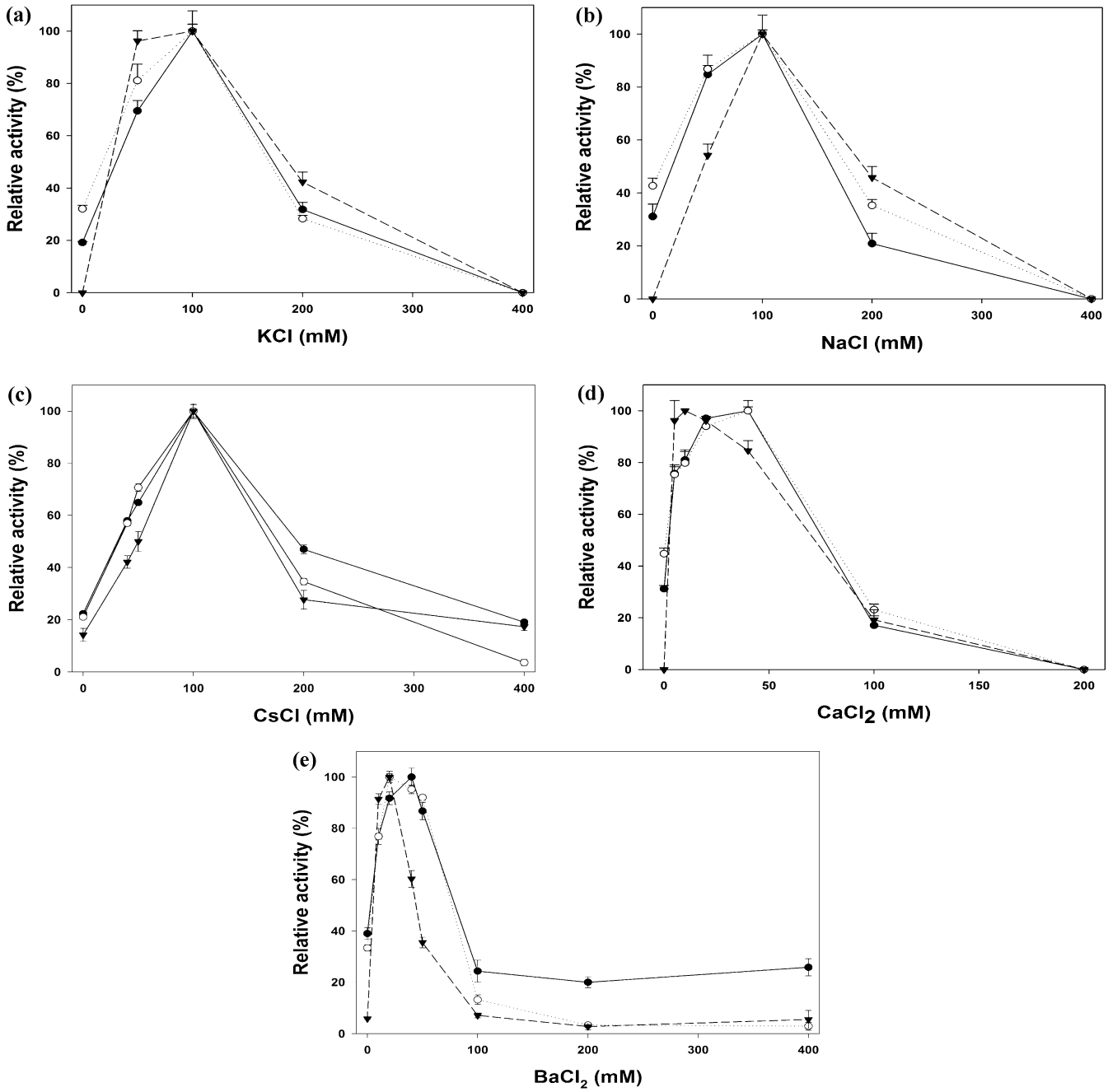

FIGURE 4: Influence of ionic concentration on BactnABC activity. Increasing concentrations of (a) KCl, (b) NaCl, (c) CsCl, (d) $CaCl_2$, and (e) $BaCl_2$ in 50 mM Tris-HCl at pH 7.6. The mixture contained 1 mg of CS-A (●, full lines), CS-C (○, dotted lines), DS (▼, dashed lines), and 0.5 μg, 1.0 μg, 1.5 μg BactnABC, respectively, in 1 mL volume.

or a glutamine in order to evaluate the importance of their cognate hydrogen bonds in catalysis. While the H344N mutant retained 5−25% catalytic efficiency toward all substrates, the H344Q mutant showed a very low k_{cat}/K_M (~5% compared to wt) only toward CS-A (Table 3). His345 mutants behaved differently. Both H345N and H345Q mutants displayed low levels of activity toward CS substrates (2−15% k_{cat}/K_M compared to wt) but no activity toward DS (Table 3 and Figure 7), suggesting that His345 plays an active role in DS catalysis.

DISCUSSION

Comparison of BactnABC with P. vulgaris Chondroitin Lyases ABC. BactnABC displays low sequence identity with the two isoforms of chondroitinase ABC from *Proteus vulgaris*. It is somewhat more similar to PvulABCII (30% identity) than to PvulABCI (23% identity). The *P. vulgaris* enzymes are well characterized (*16, 17, 27, 28*) and have found a variety of applications as analytical tools in the identification and analysis of GAG samples. More recently, this class of enzymes showed promise in the treatment of spinal cord injury (*13, 14*). Therefore, it merits comparing the properties of BactnABC to the *P. vulgaris* enzymes and investigating the biochemical conditions for their optimal activity *in vitro*.

It is noteworthy that the C-terminal, β-sheet domain of BactnABC also shows a recognizable structural similarity, albeit with low sequence identity, to the C-terminal domains of chondroitinases AC and hyaluronan lyases (*19*).

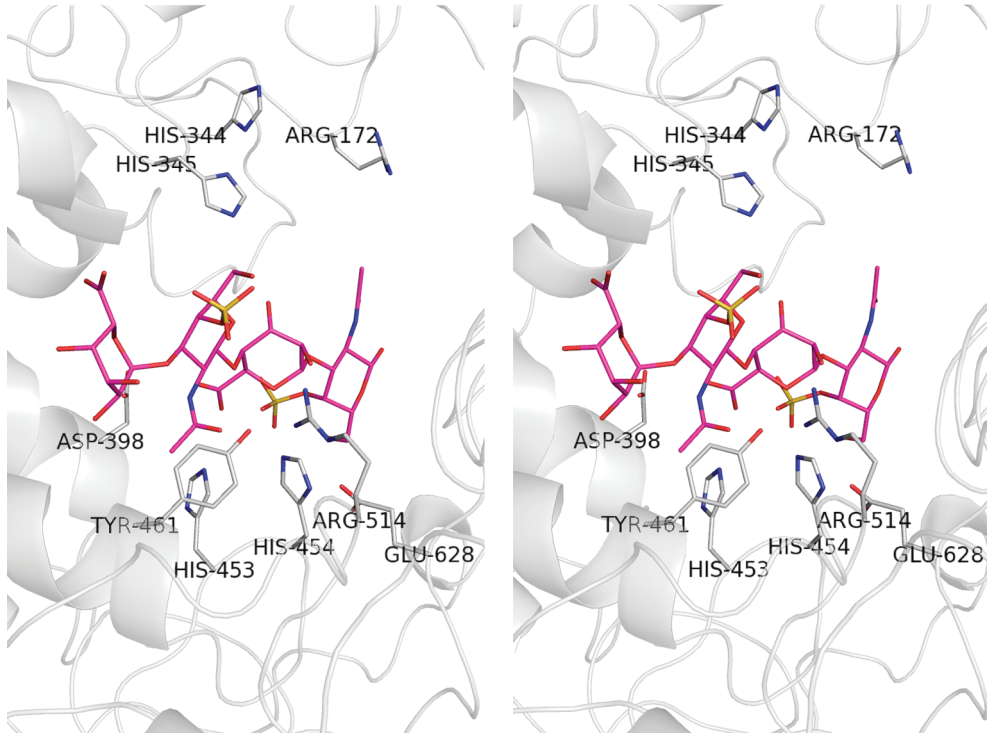

FIGURE 5: Stereo view of the active site with a modeled DS tetrasaccharide substrate. The dermatan sulfate tetrasaccharide substrate is modeled on the basis of structural superposition of the Tyr-His-Glu-Arg catalytic tetrads of BactnABC and *P. heparinus* chondroitinase AC−DS complex (PDB code 1HM2). BactnABC sidechains discussed in this work are depicted as white sticks and DS tetrasaccharide substrate as pink sticks.

Clear differences in behavior between BactnABC and PvulABCI were noted regarding the buffer conditions for their optimal enzymatic activity. While BactnABC displays optimal activity in phosphate buffer, particularly with DS as substrate, PvulABCI shows optimal activity in Tris buffer and has reduced activity toward CS-A in phosphate buffer (*17, 28*). The effect of ions for both *B. thetaiotaomicron* and *P. vulgaris* chonABC enzymes is similar (*17*). Both enzymes attain maximal activity in the presence of 0.1 M monovalent ions, whereas at 0.4 M salt completely inactivates the enzymes.

Substrate preferences of GAG lyases are usually evaluated using naturally occurring GAGs because of the lack of homogeneously modified polysaccharides (*9, 29*). We have measured the activity of *B. thetaiotaomicron* enzyme using a variety of GAGs from different suppliers and sources. BactnABC and PvulABCI share a similar preference profile toward various GAG substrates, with specific activities decreasing in the order CS-A > CS-C > DS > CS-E, CS-D ≫ HA (Table 1) (*17*). Additional information about the preference for 4- or 6-sulfation can be extracted from the differences in specific activities toward similar substrates from different suppliers (Table 1). The disaccharide compositional analysis in various GAG substrates clearly shows a preference of BactnABC for chondroitin with 4-sulfation relative to 6-sulfation, while a nonsulfated dermatan is prefered.

In comparison to PvulABCI, the respective activities of BactnABC are lower toward DS, higher toward CS-E, and lower toward HA. BactnABC depolymerization of GAGs yielded only disaccharide products, indicating an exolytic mode of action, as was shown for PvulABCII (*16*). In contrast, the products released by the endolytic PvulABCI were a mixture of tetrasaccharides and disaccharides (*17*). Thus, the higher sequence similarity of BactnABC to PvulABCII and the shared mode of action show that these two enzymes are functional homologues.

Since *B. thetaiotaomicron* resides in the human gut, the enzyme's optimum activity toward all substrates at 37 °C was expected. BactnABC displays higher thermal stability and activity at temperatures above the optimal 37 °C, as compared to PulABCI. The enzymatic activity of BactnABC was unaffected by incubation at temperatures as high as 40 °C. It retains significant activity toward CS-A, DS, and CS-C at 45 μC (Figure 2a); however, the activity drops down with preincubation, indicating partial denaturation at this temperature. PvulABCI retains only 10% of its maximal activity toward CS-C and less than 40% activity toward DS at that temperature (*17*). BactnABC displays higher apparent T_m for thermal denaturation of 44 °C as apposed to 38 °C measured for PvulABC.

The narrow pH activity profile of BactnABC reflects the importance of the protonation state of ionizable groups identified in the active site, including His344, His345, His453, His454, and Tyr461. These residues might participate in general acid/base catalysis or take part in precise hydrogen-bonding networks important for the correct positioning of active site residues. Both roles would be affected by the protonation state of these amino acids as demonstrated by the His344 and His345 mutant enzymes. Furthermore, the bell shape of the pH profile attests to the general base/acid catalytic functions discussed below for the histidine and tyrosine side chains. The marked decrease in activity below pH 6.5 is consistent with the need for the deprotonated histidine side chain acting as a general base, whereas the

Table 3: Kinetic Analysis of BactnABC and Its mutants[a]

	CS-A[b,c]			CS-C[b,d]			DS[b,e]		
enzyme	K_M (μM)	k_{cat} (min^{-1})	k_{cat}/K_M (μM$^{-1}\cdot$min^{-1})	K_M (μM)	k_{cat} (min^{-1})	k_{cat}/K_M (μM$^{-1}\cdot$min^{-1})	K_M (μM)	k_{cat} (min^{-1})	k_{cat}/K_M (μM$^{-1}\cdot$min^{-1})
WT	67 ± 1	15792 ± 238	237.5	33 ± 3	10404 ± 38	321.1	61 ± 8	2307 ± 190	38.3
H453N	34 ± 1	789 ± 34	23.2	12 ± 0.5	413 ± 17	33.8	n.d.[f]	n.d.[f]	n.d.[f]
H454/D/N/Q	**n.d.**[f]	**n.d.**[f]	**n.d.**[f]	**n.d.**[f]	**n.d.**[f]	**n.d.**[f]	**n.d.**[f]	**n.d.**[f]	**n.d.**[f]
Y461A	**n.d.**[f]	**n.d.**[f]	**n.d.**[f]	**n.d.**[f]	**n.d.**[f]	**n.d.**[f]	**n.d.**[f]	**n.d.**[f]	**n.d.**[f]
E628D	**n.d.**[f]	**n.d.**[f]	**n.d.**[f]	**n.d.**[f,g]	**n.d.**[f,g]	**n.d.**[f,g]	**n.d.**[f]	**n.d.**[f]	**n.d.**[f]
E628Q	**158 ± 25**	**623 ± 11**	**4**	**35 ± 5**	**265 ± 39**	**7.6**	**n.d.**[f]	**n.d.**[f]	**n.d.**[f]
H344D	n.d.[f,g]	n.d.[f,g]	n.d.[f,g]	n.d.[d,g]	n.d.[d,g]	n.d.[d,g]	n.d.[f]	n.d.[f]	n.d.[f]
H344E	n.d.[d,g]	n.d.[f,g]	n.d.[f,g]	n.d.[f]	n.d.[f]	n.d.[f]	n.d.[f]	n.d.[f]	n.d.[f]
H344N	39 ± 0.4	2532 ± 70	64.8	84 ± 18	1122 ± 66	13.7	90 ± 5	544 ± 10	6.1
H344Q	73 ± 3	1007 ± 91	13.8	n.d.[f,g]	n.d.[f,g]	n.d.[f,g]	n.d.[f]	n.d.[d]	n.d.[f]
H345D/E	n.d.[f,g]	n.d.[f,g]	n.d.[f]	n.d.[f]	n.d.[f]	n.d.[f]	n.d.[f]	n.d.[d]	n.d.[f]
H345N	61 ± 5	1260 ± 40	20.6	26 ± 0.1	396 ± 14	15.1	n.d.[d]	n.d.[d]	n.d.[f]
H345Q	45 ± 4	1408 ± 144	31.3	102 ± 6	651 ± 61	6.4	n.d.[d]	n.d.[f]	n.d.[f]

[a] Mutants of the tetrad residues are in bold font. [b] Results are the mean ± SD for at least three measurements. [c] 1 mg mL^{-1} CS-A from bovine trachea (Biocorp) in 50 mM phosphate buffer at pH 7.6, measured for 300 s at 37 °C using 0.5 μg of enzyme. [d] 1 mg mL^{-1} CS-C from shark cartilage (sigma) in 50 mM phosphate buffer at pH 7.6, measured for 300 s at 37 °C using 1.0 μg of enzyme. [e] 1 mg mL^{-1} DS from porcine intestinal mucosa (sigma) in 50 mM phosphate buffer at pH 7.6, measured for 300 s at 37 °C using 1.5 μg of enzyme. [f] n.d., not detected. [g] Showed residual activity on the overnight degradation at 37 °C, but the values were too low for kinetic calculations.

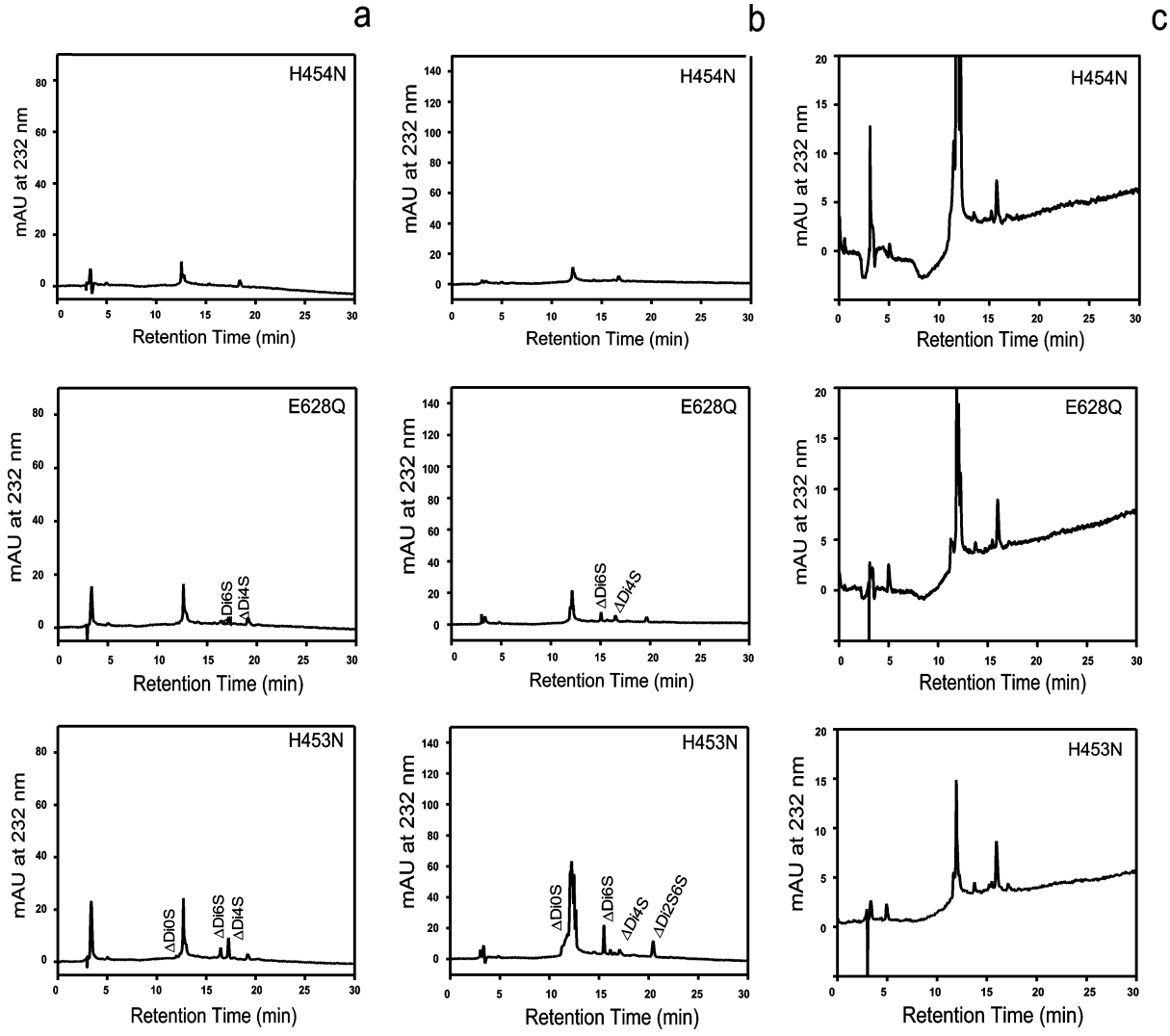

FIGURE 6: Product profile analysis using SAX-FPLC for BactnABC mutants of the tetrad residues H454N, E628Q, and H453N acting on (a) Biocorp CS-A, (b) Sigma CS-C, and (c) Sigma DS. Identified disaccharides are marked as in Figure 3.

low activity recorded above pH 8.5 is consistent with the importance of a protonated tyrosine acting as a general acid.

Toward Understanding the Catalytic Mechanism. Of the five divalent cations tested, Ca^{2+}, Mg^{2+}, and Ba^{2+} increase the specific activity of BactnABC toward all substrates, whereas Zn^{2+} and Mn^{2+} decrease the activity against CS while mildly increasing the activity toward DS. Ca^{2+}/Ba^{2+} cations affect the catalytic activity toward CS in a different

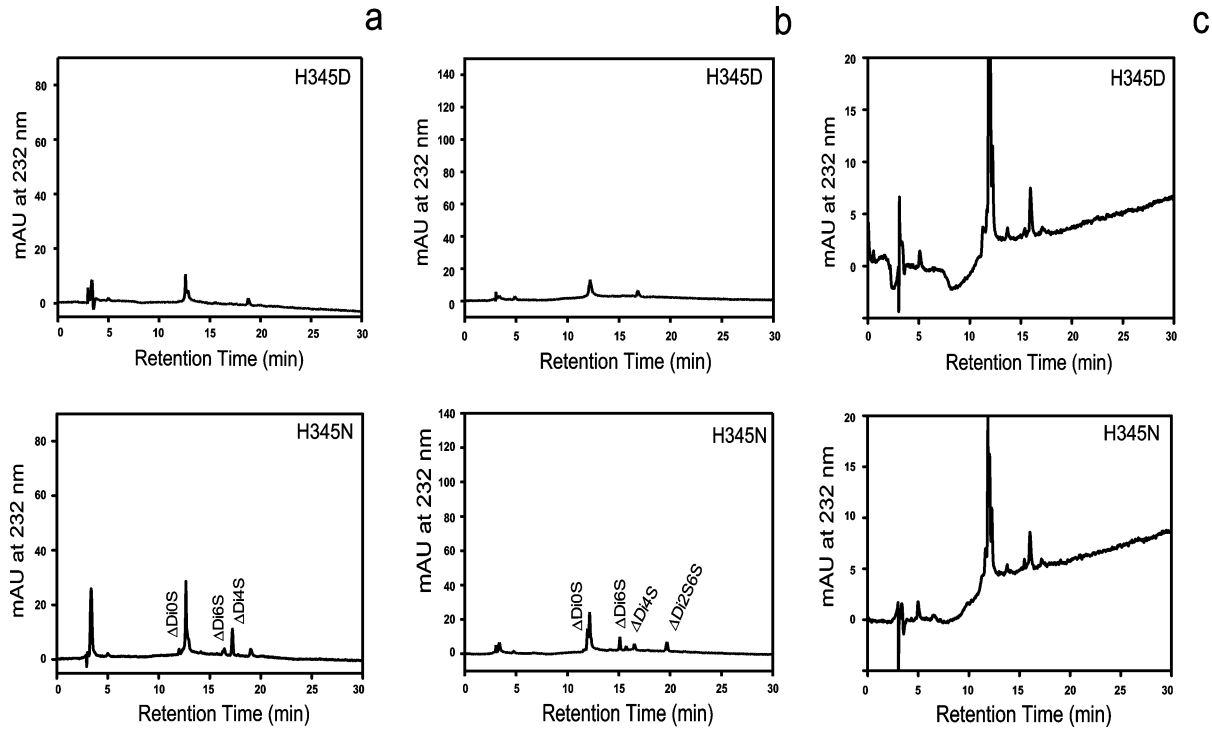

FIGURE 7: Mutants of the second active site H345D/N acting on (a) Biocorp CS-A, (b) Sigma CS-C, and (c) Sigma DS. Identified disaccharides are marked as in Figure 3.

manner than toward DS. The effect on CS is predominantly related to ionic strength in a fashion similar to that exerted by the monovalent salts (Figure 4). However, the activity toward DS is dramatically augmented in the presence of divalent cations, with maximal effect at a much lower ion concentration, indicating selective differences in the effect of the metal in the degradation of these two substrates. This behavior is reminiscent of the narrower specificity lyases, chondroitinase AC and chondroitinase B. These two enzymes present different three-dimensional folds and catalytic site arrangements (*26, 30–32*). Chondroitinase AC requires no divalent cations to degrade CS, while chondroitinase B requires the presence of Ca^{2+} to break down DS. The Ca^{2+} is coordinated between the enzyme and the iduronic acid moiety of DS, neutralizing the negative charge of the acidic group (*32*). We propose that BactnABC requires a metal cation for binding DS, whereas it is not necessary for the binding of CS. Furthermore, we propose that BactnABC uses the metal to neutralize the negative charge of the IdoA carboxylate moiety, as has been found for DS in chondroitinase B. This effect is metal-specific, as neither Zn^{2+} nor Mn^{2+} enhance the activity significantly toward DS.

The β-elimination reaction mechanism requires charge neutralization of the negative carboxylic group of the uronic acid in order to reduce the p*K*a of the C5-bound proton (*11*). The next step of catalysis involves a residue acting as a general base, triggering the elimination by removal of the C5 proton from the uronic acid with the formation of a C4−C5 double bond in the uronic acid ring. Concomitantly or subsequently, an amino acid acting as a general acid protonates the bridging oxygen between the uronic acid and glucosamine, thus breaking the glycosidic bond, completing the degradation and releasing the products (*11*).

We have previously postulated that substrate binding involves a conformational rearrangement, bringing the tetrad and residues on the opposite rim of the binding site into proximity, creating one composite active site with different side chains participating in the consecutive reaction steps for different substrates (*19*).

In addition to the alanine replacements other, more conservative mutations of the tetrad components inactivated the enzyme toward all substrates. An exception is the E628Q mutant, which retained a low catalytic efficiency toward CS substrates. The low tolerance for chemical changes in the tetrad implies the importance of a precise hydrogen-bonding network between the residues comprising the tetrad. The specific interactions between those residues are vital for correct placement of the chemical groups necessary for the degradation to take place. The acute influence of the tetrad residues on the degradation of both substrates indicates that these residues take part in the final step of degradation−proton donation and product release, which we propose is shared by both substrates. In the case of CS degradation, the tetrad residues are proposed to function in the first step of degradation as well, paralleling chondroitinase AC (*30*). The lack of activity for all mutants of either His454 or Tyr461 does not permit distinguishing which residue acts as the general base abstracting the C5 proton from the glucuronic acid of CS. The low catalytic efficiency of the E628Q mutant is in agreement with the chondroitinase AC crystal structure (*30*), which showed that Glu628 is important for the positioning of Arg514 and His454 rather than being directly involved in catalysis. The replacement of Glu628 by a glutamine would preserve the hydrogen bonds to Arg514 and His454, although to the latter only in its neutral state. The generally low activity of BactnABC in the acidic range may therefore be related in part to the protonation of this glutamate residue, mimicking glutamine in this position.

The H453N mutant shows no activity toward DS, while retaining about 10% of its catalytic efficiency against CS-A

and CS-C. This decrease is mostly related to a reduction of k_{cat} for these substrates. Comparing the BactnABC crystal structure (PDB code 2Q1F) to chondroitinase AC−CS tetrasaccharide complex (PDB code 1RWH), we find the side chain of His453 located close to the predicted location of the uronate carboxylic group. We suggest that this histidine is involved in charge neutralization for CS and DS substrates, either directly, by hydrogen bonding to the carboxylic group in CS degradation, or indirectly, by coordinating the Ca^{2+} (possibly with Asp398) in DS degradation.

We have previously demonstrated by alanine mutations that His344 and His345 play key roles in DS degradation but are not absolutely essential for degradation of CS (*19*). Replacement of His345 by either asparagine or glutamine had a similar effect as the alanine replacement; the mutants are inactive toward DS, while the catalytic efficiency toward CS decreases to 5−10% of the wild type enzyme. Therefore, a histidine side chain with its potential to abstract a proton, rather than asparagine or glutamine, with nitrogen atoms isosteric to the histidine nitrogen atoms, is essential for DS degradation. His344 plays a different role. The H344N mutant retains ∼5−25% catalytic efficiency toward all substrates, while H344Q displays low levels of activity only toward CS-A but not toward CS-C or DS. Therefore, asparagine but not glutamine can partially replace His344, indicating that the ND nitrogen of His344 is important. Indeed, in the crystal structure (PDB code 2Q1F) this nitrogen atom is involved in a hydrogen bond to His345, likely anchoring the latter in a proper orientation for catalysis. Finally, mutation of either of these two histidines to an acidic residue, aspartate or glutamate, inactivates the enzyme toward all substrates. This substitution introduces a negative charge in the substrate binding site and most likely adversely affects binding of the highly negatively charged substrates. Together, the kinetic properties of the site-specific mutants suggest that with CS as a substrate these two histidines participate in substrate binding, whereas for DS, His345 serves as the catalytic base, and His344 is essential for maintaining the correct positioning and specific protonation of His345.

Our results provide additional support for the notion of a composite active site in BactnABC, allowing for the degradation of GAGs possessing both uronic acid epimers. The residue that performs the first step of degradation, proton abstraction from the C5 carbon, is different for CS (GlcA-containing) than for the DS (IdoA-containing) substrate as a result of the difference in configuration of the substituents of the C5 carbon. In contrast, proton donation to the leaving group involves a planar intermediate common for both epimers, and consequently, the same residue can carry out the reaction with either substrate. The tetrad participates in both acid and base catalysis for CS but only in donating a proton to the leaving group with DS as substrate. His345 from the rim of the substrate binding cleft opposite to the tetrad was identified as the most likely candidate for proton abstraction of DS substrate. In addition, we provide a comprehensive biochemical characterization of BactnABC, establishing optimal conditions for *in vitro* degradation of CS-A, CS-C, and DS.

ACKNOWLEDGMENT

We thank Drs. Holger Lindner and Allan Matte for their helpful comments when preparing this manuscript.

SUPPORTING INFORMATION AVAILABLE

The primer sequences, the amino acid sequence of BactnABC, and the SAX-FPLC product analysis for the mutants described in the text. This material is available free of charge via the Internet at http://pubs.acs.org.

REFERENCES

1. Iozzo, R. V., and Cohen, I. (1993) Altered proteoglycan gene expression and the tumor stroma. *Experientia 49*, 447–455.
2. Varki, A. (1993) Biological roles of oligosaccharides: all of the theories are correct. *Glycobiology 3*, 97–130.
3. Iozzo, R. V. (1998) Matrix proteoglycans: from molecular design to cellular function. *Annu. Rev. Biochem. 67*, 609–652.
4. Lander, A. D., and Selleck, S. B. (2000) The elusive functions of proteoglycans: in vivo veritas. *J. Cell Biol. 148*, 227–232.
5. Sugahara, K., and Kitagawa, H. (2000) Recent advances in the study of the biosynthesis and functions of sulfated glycosaminoglycans. *Curr. Opin. Struct. Biol. 10*, 518–527.
6. Trowbridge, J. M., and Gallo, R. L. (2002) Dermatan sulfate: new functions from an old glycosaminoglycan. *Glycobiology 12*, 117R–125R.
7. Sugahara, K., Mikami, T., Uyama, T., Mizuguchi, S., Nomura, K., and Kitagawa, H. (2003) Recent advances in the structural biology of chondroitin sulfate and dermatan sulfate. *Curr. Opin. Struct. Biol. 13*, 612–620.
8. Bao, X., Nishimura, S., Mikami, T., Yamada, S., Itoh, N., and Sugahara, K. (2004) Chondroitin sulfate/dermatan sulfate hybrid chains from embryonic pig brain, which contain a higher proportion of L-iduronic acid than those from adult pig brain, exhibit neuritogenic and growth factor binding activities. *J. Biol. Chem. 279*, 9765–9776.
9. Ernst, S., Langer, R., Cooney, C. L., and Sasisekharan, R. (1995) Enzymatic degradation of glycosaminoglycans. *Crit. Rev. Biochem. Mol. Biol. 30*, 387–444.
10. Valla, S., Li, J., Ertesvag, H., Barbeyron, T., and Lindahl, U. (2001) Hexuronyl C5-epimerases in alginate and glycosaminoglycan biosynthesis. *Biochimie 83*, 819–830.
11. Gacesa, P. (1987) Alginate-modifying enzymes. A proposed unified mechanism of action for the lyases and epimerases. *FEBS Lett. 212*, 199–202.
12. Aguiar, J. A., Lima, C. R., Berto, A. G., and Michelacci, Y. M. (2003) An improved methodology to produce *Flavobacterium heparinum* chondroitinases, important instruments for diagnosis of diseases. *Biotechnol. Appl. Biochem 37*, 115–127.
13. Bradbury, E. J., Moon, L. D., Popat, R. J., King, V. R., Bennett, G. S., Patel, P. N., Fawcett, J. W., and McMahon, S. B. (2002) Chondroitinase ABC promotes functional recovery after spinal cord injury. *Nature 416*, 636–640.
14. Lemons, M. L., Sandy, J. D., Anderson, D. K., and Howland, D. R. (2003) Intact aggrecan and chondroitin sulfate-depleted aggrecan core glycoprotein inhibit axon growth in the adult rat spinal cord. *Exp. Neurol. 184*, 981–990.
15. Linn, S., Chan, T., Lipeski, L., and Salyers, A. A. (1983) Isolation and characterization of two chondroitin lyases from *Bacteroides thetaiotaomicron*. *J. Bacteriol. 156*, 859–866.
16. Hamai, A., Hashimoto, N., Mochizuki, H., Kato, F., Makiguchi, Y., Horie, K., and Suzuki, S. (1997) Two distinct chondroitin sulfate ABC lyases. An endoeliminase yielding tetrasaccharides and an exoeliminase preferentially acting on oligosaccharides. *J. Biol. Chem. 272*, 9123–9130.
17. Prabhakar, V., Capila, I., Bosques, C. J., Pojasek, K., and Sasisekharan, R. (2005) Chondroitinase ABC I from *Proteus vulgaris*: cloning, recombinant expression and active site identification. *Biochem. J. 386*, 103–112.
18. Huang, W., Lunin, V. V., Li, Y., Suzuki, S., Sugiura, N., Miyazono, H., and Cygler, M. (2003) Crystal structure of *Proteus vulgaris* chondroitin sulfate ABC lyase I at 1.9A resolution. *J. Mol. Biol. 328*, 623–634.
19. Shaya, D., Hahn, B. S., Bjerkan, T. M., Kim, W. S., Park, N. Y., Sim, J. S., Kim, Y. S., and Cygler, M. (2008) Composite active site of chondroitin lyase ABC accepting both epimers of uronic acid. *Glycobiology 18*, 270–277.
20. Yamagata, T., Saito, H., Habuchi, O., and Suzuki, S. (1968) Purification and properties of bacterial chondroitinases and chondrosulfatases. *J. Biol. Chem. 243*, 1523–1535.

21. Kim, Y. S., Jo, Y. Y., Chang, I. M., Toida, T., Park, Y., and Linhardt, R. J. (1996) A new glycosaminoglycan from the giant African snail *Achatina fulica*. *J. Biol. Chem. 271*, 11750–11755.
22. Matulis, D., Kranz, J. K., Salemme, F. R., and Todd, M. J. (2005) Thermodynamic stability of carbonic anhydrase: measurements of binding affinity and stoichiometry using ThermoFluor. *Biochemistry 44*, 5258–5266.
23. Vedadi, M., Niesen, F. H., lali-Hassani, A., Fedorov, O. Y., Finerty, P. J., Jr., Wasney, G. A., Yeung, R., Arrowsmith, C., Ball, L. J., Berglund, H., Hui, R., Marsden, B. D., Nordlund, P., Sundstrom, M., Weigelt, J., and Edwards, A. M. (2006) Chemical screening methods to identify ligands that promote protein stability, protein crystallization, and structure determination. *Proc. Natl. Acad. Sci. U.S.A 103*, 15835–15840.
24. Lo, M. C., Aulabaugh, A., Jin, G., Cowling, R., Bard, J., Malamas, M., and Ellestad, G. (2004) Evaluation of fluorescence-based thermal shift assays for hit identification in drug discovery. *Anal. Biochem. 332*, 153–159.
25. Huang, W., Boju, L., Tkalec, L., Su, H., Yang, H. O., Gunay, N. S., Linhardt, R. J., Kim, Y. S., Matte, A., and Cygler, M. (2001) Active site of chondroitin AC lyase revealed by the structure of enzyme-oligosaccharide complexes and mutagenesis. *Biochemistry 40*, 2359–2372.
26. Féthière, J., Eggimann, B., and Cygler, M. (1999) Crystal structure of chondroitin AC lyase, a representative of a family of glycosaminoglycan degrading enzymes. *J. Mol. Biol. 288*, 635–647.
27. Prabhakar, V., Capila, I., Raman, R., Srinivasan, A., Bosques, C. J., Pojasek, K., Wrick, M. A., and Sasisekharan, R. (2006) The catalytic machinery of chondroitinase ABC I utilizes a calcium coordination strategy to optimally process dermatan sulfate. *Biochemistry 45*, 11130–11139.
28. Prabhakar, V., Raman, R., Capila, I., Bosques, C. J., Pojasek, K., and Sasisekharan, R. (2005) Biochemical characterization of the chondroitinase ABC I active site. *Biochem. J. 390*, 395–405.
29. Sasisekharan, R., Raman, R., and Prabhakar, V. (2006) Glycomics approach to structure-function relationships of glycosaminoglycans. *Annu. Rev. Biomed. Eng 8*, 181–231.
30. Lunin, V. V., Li, Y., Linhardt, R. J., Miyazono, H., Kyogashima, M., Kaneko, T., Bell, A. W., and Cygler, M. (2004) High resolution crystal structure of *Arthrobacter aurescens* chondroitin AC lyase: enzyme-substrate complex defines the catalytic mechanism. *J. Mol. Biol. 337*, 367–386.
31. Huang, W., Matte, A., Li, Y., Kim, Y. S., Linhardt, R. J., Su, H., and Cygler, M. (1999) Crystal structure of chondroitinase B from *Flavobacterium heparinum* and its complex with a disaccharide product at 1.7Å resolution. *J. Mol. Biol. 294*, 1257–1269.
32. Michel, G., Pojasek, K., Li, Y., Sulea, T., Linhardt, R. J., Raman, R., Prabhakar, V., Sasisekharan, R., and Cygler, M. (2004) The structure of chondroitin B lyase complexed with glycosaminoglycan oligosaccharides unravels a calcium-dependent catalytic machinery. *J. Biol. Chem. 279*, 32882–32896.

BI800353G